

Competition for water and species coexistence in phenologically structured annual plant communities

Jacob I. Levine¹  | Jonathan M. Levine¹  | Theo Gibbs²  | Stephen W. Pacala¹

¹Department of Ecology and Evolutionary Biology, Princeton University, Princeton, New Jersey, USA

²Lewis-Sigler Institute for Integrative Genomics, Princeton University, Princeton, New Jersey, USA

Correspondence

Jacob I. Levine, Department of Ecology and Evolutionary Biology, Guyot Hall, Princeton University, Princeton, NJ, USA.
Email: jacolevine@princeton.edu

Editor: Johannes Knopss

Abstract

Both competition for water and phenological variation are important determinants of plant community structure, but ecologists lack a synthetic theory for how they affect coexistence outcomes. We developed an analytically tractable model of water competition for Mediterranean annual communities and demonstrated that variation in phenology alone can maintain high diversity in spatially homogenous assemblages of water-limited plants. We modelled a system where all water arrives early in the season and species vary in their ability to grow under drying conditions. As a consequence, species differ in growing season length and compete by shortening the growing season of their competitors. This model replicates and offers mechanistic explanations for patterns observed in empirical studies of how phenology influences coexistence among Mediterranean annuals. Additionally, we found that a decreasing, concave-up trade-off between growth rate and access to water can maintain high diversity under simple but realistic assumptions. High diversity is possible because: (1) later plants escape competition after their earlier season competitors have gone to seed and (2) early-season species are more than compensated for their shortened growing season by a growth rate advantage. Together, these mechanisms provide an explanation for how phenologically variable annual plant species might coexist when competing only for water.

KEY WORDS

annual plants, coexistence, ecohydrology, ecophysiology, phenology, water competition

INTRODUCTION

Competition for water is an important driver of plant community structure globally (Craine & Dybzinski, 2013; Goldberg & Novoplansky, 2009; Rosenzweig, 1968; Schwinnig & Kelly, 2013), yet ecologists lack synthetic theory for how species coexist on limited water resources (Craine & Dybzinski, 2013). In place of such theory, community ecologists often use generic consumer-resource models with an abiotic 'resource' to understand and predict the outcome of water competition among plants (Seabloom et al., 2003). However, the use of these models might miss critical aspects of plant competition that uniquely emerge when species compete for water. Indeed, past empirical studies suggest that

while consumer-resource models adequately predict the coexistence and competitive dynamics of plants competing for soil nutrients, unexpected dynamics can emerge when plants compete for water (Farrar et al., 2013). For example, Farrar et al. (2013) predicted and empirically verified that additional nitrogen decreases a plant's allocation to roots, but that water addition increases root allocation. This dynamic would be missed in a generic consumer-resource modelling framework. Properly understanding coexistence when plants compete for water would seemingly require integrating over (1) the temporally variable physical factors that affect water availability; (2) the physiological relationships between water availability and plant growth and mortality and (3) demography, the net result of variable plant growth

and death rates over time (Daly et al., 2004; Rodriguez-Iturbe & Porporato, 2007). However, when integrated across multiple competing species, these processes result in intractable, highly non-linear dynamics.

Recent advances in ecohydrology (Box 1) simplify the problem considerably and thereby facilitate the development of tractable models of the coexistence of plant species competing for water. Specifically, the equations governing stomatal behaviour (Ball et al., 1987; Sperry et al., 2016; Wolf et al., 2016) show that stomatal aperture, and therefore biomass growth, is virtually independent of soil water until soil becomes drier than a species-specific threshold. At this point, a plant's biomass growth rate and soil water depletion feedback on one another, rendering models of biomass growth mathematically intractable. This remains true until biomass growth falls to zero at a species-specific threshold minimum water availability. What ultimately makes this dynamic tractable is the recent discovery that the period of water-limited growth is short enough to be ignored for most competition problems. Specifically, when limited by water, plants run the risk of embolism, which if severe, greatly reduces water transport and depresses xylem water potential. To avoid these costs, plants tend to shut stomates well before substantial embolism risk occurs (Anderegg et al., 2016; Farquhar & Sharkey, 1982; Sala et al., 2012; Tyree & Sperry, 1989; Wolf et al., 2016), effectively truncating the period of water-limited growth. As a result, the relationship between biomass growth rate and soil water availability can be safely approximated as a simple step function – plants grow uninhibited above some species-specific threshold water availability and stop growing below that threshold, a value we call a plant species' 'shut-off point' (Box 1; Appendix 1).

Here, we show how the phenological structuring of plant communities that emerges when water is seasonally pulsed and species differ in their shut-off points enables the coexistence of plant competitors. Specifically, species with costly to produce thick-walled xylem and high allocation to roots grow longer under drier conditions than species with opposing traits, as these features help plants avoid embolism. Because roots and thick-walled xylem are made at the expense of productive leaves, this creates a trade-off between biomass growth rate and the minimum soil water availability at which a species can continue to grow (Enquist et al., 1999; Hacke et al., 2001; Rosner, 2017). This trade-off then sorts species in time. When the soil is wet, the fastest growing species build biomass, and hence future fecundity, more rapidly than any other species. But, it then stops growing before all others as the soil dries, leaving a period of growth for species able to transpire (and continue to grow) at low water potentials (Appendix 4.2). In sum, interspecific variation in tolerance to low water availability, combined with temporal variation in water supply, means that successively smaller subsets of species are actively growing as the season progresses and water is depleted.

Although exactly how this phenological structuring maintains plant species diversity is only beginning to be explored in mechanistic models, we have good reason to believe that phenological variation, driven by water or otherwise, plays a significant role in plant coexistence. We commonly observe large phenological diversity in plant communities throughout the world (Craine et al., 2012; Rathcke & Lacey, 1985). Moreover, phenological differences between species determine the outcome of interactions between invasive and resident plant species (Fridley, 2012; Godoy & Levine, 2014) and the overyielding potential in diverse communities (Hooper & Dukes, 2010). Patterns such as these have motivated past verbal models of how phenological variation influences ecological dynamics, invoking concepts such as phenological niches and niche pre-emption (Wolkovich & Cleland, 2011). Since then, studies have combined empirical work with coexistence theory (Chesson, 2000) to explore how phenological differences relate to the niche differences that stabilise coexistence and the competitive imbalances that drive the exclusion of inferior competitors (Alexander & Levine, 2019; Godoy & Levine, 2014). However, this phenomenological modelling approach relies on high-level abstractions of the competitive process and does not identify the source of the interactions enabling coexistence. Thus, a detailed, physiologically grounded model might clarify the processes by which phenological structuring in water-limited communities influences competitive outcomes.

In this paper, we develop theory informed by ecohydrology to answer the following questions: (1) Can trade-offs associated with water competition explain the high diversity observed in phenologically structured plant communities in nature? (2) Under what conditions do these mechanisms foster coexistence versus competitive exclusion?

We examine these questions by modelling a system with relatively simple water dynamics, demography and phenological structure: Mediterranean annual plant assemblages. In these assemblages, a period of winter rainfall and abundant water is followed by a warmer dry period of water limitation, after which, plants successively die. These simplifying features of the hydrology are important because the complexity in the inputs and losses of water that characterise most other systems makes modelling competition for water particularly challenging (Daly et al., 2004; Rodriguez-Iturbe & Porporato, 2007). For example, on the input side in most systems, precipitation comes in the form of storm events, which vary stochastically in their intensity, frequency and duration (Pilar Fernandez-Illescas & Rodriguez-Iturbe 2003; Rodriguez-Iturbe & Porporato, 2007). Systems dependent on stochastic, pulsed inputs interspersed with periods of water limitation make challenging subjects for modelling competition.

By contrast, in Mediterranean annual systems, germination is induced at the start of a relatively short 3–4-month winter rainy season, and the majority of



BOX 1 Ecophysiology relevant to the modelled dependence of biomass growth on soil water

Photosynthesis requires a continuous supply of water as controlled by a plant's stomatal conductance, $g = \frac{y}{D_s} (\psi_{soil} - \psi_{leaf})$, where y is the ratio of root area to leaf area, k is the plant's xylem conductivity and D_s is a measure of air moisture content (vapour pressure deficit). For stomatal conductance g , and therefore photosynthesis, to remain positive, there must be a positive gradient between soil water potential, ψ_{soil} , and a plant's leaf water potential, ψ_{leaf} (Farquhar & Sharkey, 1982). Therefore, as soil water potential drops throughout the season due to loss of soil moisture via transpiration, a plant's leaf water potential, ψ_{leaf} , must also drop to maintain a positive gradient. However, ψ_{leaf} can only reduce to a certain value before embolism risk becomes high. To protect against embolism, plants have an internal shut-off mechanism, $\beta(\psi_{leaf})$, which closes stomates, reducing stomatal conductance in order to keep ψ_{leaf} at a safe level, ψ^* (Wolf et al., 2016). The value of ψ^* is typically buffered against values for which embolism is a severe risk and is primarily determined by a plant's physiological characteristics (Daly et al., 2004; Manzoni et al., 2011). Above ψ^* , the gradient between leaf and soil water potential is large enough that photosynthesis is not water limited — meaning the plant accumulates carbon at its maximum rate, a_{max} , which is determined by light availability and the plant's internal carbon concentration (Farquhar & Sharkey, 1982; Leuning, 1995). Once $\psi_{leaf} = \psi^*$, ψ_{leaf} remains fixed, photosynthesis becomes water limited and carbon accumulation, a , drops until the soil water potential also equals ψ^* at which point the plant stops growing (Figure S1).

In the period between when ψ_{leaf} first reaches ψ^* and when the plant shuts down, the dependence of a plant's growth rate of water content causes demographic models of water-limited plants to be intractable. However, several considerations lead to a simple approximation. First, a plant's carbon accumulation rate is a function of stomatal conductance which is itself a function of both the plant's carbon accumulation rate and $\beta(\psi_{leaf})$ (Farquhar & Sharkey, 1982; Leuning, 1995). The dependence of the carbon accumulation rate on the carbon accumulation rate itself creates a positive feedback such that in the period during which $\psi_{leaf} = \psi^*$ the rate of decrease in a plant's carbon accumulation is both rapid and accelerating. Second, when plants transpire, they remove water from the soil volumetrically. Volumetric water content is related nonlinearly to soil water potential in a manner such that a given volumetric removal results in a greater reduction of soil water potential in dry conditions than in wet conditions. Additionally, a plant's transpiration rate increases as a function of plant size. Since plants are largest and soil is driest at the end of the season, the period of declining growth rate is negligible in terms of its contribution to total growth. Detailed calculations supporting this result are provided in Appendix 1.3. Having established that the declining growth rate in this period has a negligible effect on total within-season plant growth, we can safely approximate a plant's carbon accumulation rate as a step function such that $a = a_m$ when $\psi_{soil} > \psi^*$ and $a = 0$ when $\psi_{soil} \leq \psi^*$ (simulations testing the sensitivity of our results to this approximation are provided in Appendix 9.3).

As individual plants grow, they withdraw and transpire water from a common pool at a rate proportional to their leaf area, stomatal conductance and vapour pressure deficit. This relationship is given by

$$E = a_m D_s \phi \beta(\psi_{leaf}) \quad (\text{B.1})$$

where E is the rate of transpiration per unit leaf area, a_m is the maximum photosynthetic rate, internal carbon concentration and the leaf respiration cost, D_s is the vapor pressure deficit, $\beta(\psi_{leaf})$ is the shut-off operator and ϕ is a collection of physiological parameters which in addition to a_m determine stomatal conductance (see Appendix 1 for a full description of parameters). Since we are primarily interested in parsing the effects of water-limitation-induced variability in phenology, we assume that the constants in Equation (B.1) are invariable in time and among species. Thereby, species operate at their maximum photosynthetic rate until $\psi_{soil} = \psi^*$, at which point they stop growing and convert to seed. This facet of plant growth also implies that the transpiration rate per unit leaf area remains constant throughout the growing season.

1 for a full description of parameters). Since we are primarily interested in parsing the effects of water-limitation-induced variability in phenology, we assume that the constants in Equation (B.1) are invariable in time and among species. Thereby, species operate at their maximum photosynthetic rate until $\psi_{soil} = \psi^*$, at which point they stop growing and convert to seed. This facet of plant growth also implies that the transpiration rate per unit leaf area remains constant throughout the growing season.

plants grow well through this rainy season, and only complete their life cycle during the subsequent period when the water is being depleted (Levine & HilleRisLambers, 2009; Seabloom et al., 2003). The general decrease in water availability after the end of the rainy period as well as between-species variation in their tolerance to

dry conditions results in large interspecific phenological variation (Alexander & Levine, 2019; Godoy & Levine, 2014). Some species complete their life cycle in spring, while others persist through fall. This phenological variation and its association with competitive dynamics have been investigated in several past empirical studies



(Alexander & Levine, 2019; Godoy & Levine, 2014; Kraft et al., 2015), providing key real-world tests for the models we develop here.

WATER COMPETITION MODEL

We develop a general model of plants competing for water when soil water availability determines the duration of each competitor's growing season. Although we tailor the model to a community of seasonally water-limited Mediterranean annual plant species that differ in their ability to grow under dry conditions, the findings should apply more broadly. The outline of the model is as follows: Plants grow unfettered by neighbours until neighbours reduce the water content of the soil, W , to less than the species-specific minimum water content required for an individual to grow, W^* (mass of water per unit land area or volumetric water content with fixed soil depth). Individual species successively stop growing and convert biomass to seeds, and after the last species does so, the season begins again. In this section, we build a quantitative model which formalises these dynamics.

A year begins with all individuals of all species in the seed stage, and all germinate synchronously after the onset of the rainy season. We assume for simplicity that negligible water is carried over in the soil from 1 year to the next, that negligible water is lost to run-off, groundwater and evaporation from the soil (not transpiration), and that rain ceases on the day plants germinate. All of these simplifying assumptions can be relaxed without changing the qualitative results (Appendix 9).

After germination, plants grow at a constant rate (when time is measured on a non-linear scale, but at an accelerating rate in regular time) until soil water content drops below the species-specific critical value (Appendix 2). Specifically, we assume that the biomass and crown area of an individual are related by a power-law allometry with exponents common to all species. When a plant is actively growing, its rate of carbon gain is proportional to its leaf area, which implies plants do not shade one another (Appendix 1.1). This property, together with the power-law allometry imply that, at time t during the growing season, a species- i individual's biomass is approximately $(G_i t)^B$, where G_i is a species-specific constant growth rate and B is a constant common to all species (Appendix 2). Therefore, if we use the non-linear timescale $\tau = t^B$ in place of ordinal time t , individuals of species i grow at a constant species-specific rate, G_i^B , until the time at which soil water content drops below that species' critical value ($W < W^*$). We denote this time t_i or in the non-linear timescale τ_i (which equals t_i^B). Also, at this time, all individuals of species i convert their biomass ($G_i^B t_i^B$) to seeds following a proportionality constant shared across all species, and these seeds survive to initiate next year's growth process.

Competition emerges in this model only because individuals uptake and transpire the limited soil water pool and

thereby shorten the growing season lengths of competitors. The greater the abundance of conspecific or heterospecific competitors, the faster the uptake and depletion of the finite soil water pool, and the earlier soil water drops below each species' critical value. A plant's biomass accumulation rate during the period suitable for its growth, G_i^B , is unaffected by competition from other individuals (Box 1); only the duration of growth is affected by competition.

Three seemingly special assumptions make competition for water in this system analytically tractable – (1) plants have constant growth until a season's end determined by a soil water threshold, (2) competition between species shortens growing season lengths without changing growth rates during the growing season and (3) end-of-season fecundity is proportional to t_i^B , with B common to all species. Importantly, all are emergent properties of plant physiology under a simple hydraulic model (described in Box 1 and Appendix 1, 2) provided that species adhere to power-law allometry. We empirically verify this allometry, justify it theoretically and test the robustness of the model to these assumptions in Appendix 2.1, 2.2, 2.4, 9.1 and 9.3.

A single-species system

In this section, we quantitatively describe the dynamics of a single species in a water-limited system because the multispecies model follows naturally from this simpler case. To keep the notation simple, in this section, we omit the species-specific subscript from all quantities *except the season length*, τ_1 , to distinguish it from the within-year time τ . Let N_T be the population density of seeds in the soil starting year T (note: upper case "T" designates year, whereas lower case 't' or 'τ' designates time since germination within a year). Also, because growing season length is a decreasing function of population size, we write it as $\tau_1(N_T)$. We assume the number of seeds available to start the season is proportional to the prior year's end-of-season biomass according to the constant F . This yields the following expression for per capita population growth in year T

$$\frac{N_{(T+1)}}{N_T} = FG^B \tau_1(N_T). \quad (1)$$

Since both F and G^B are constants, the per capita population growth rate of species i varies solely as a function of its growing season length, τ_1 , which is itself a function of the rate at which water is withdrawn from the common pool.

Given that competition occurs through a shortening of the growing season, it is useful to define the length of the season for which the population shows zero growth. Note that the lifetime reproductive success (LRS) of a recently germinated seedling equals the expected number of germinable seeds it will produce during its lifetime, and that this increases with season length, $\tau_1(N_T)$. We call the



'break-even time' τ^* - the value of τ at which LRS equals one (or equivalently, $N_{T+1} = N_T$). By definition, $\tau_1(N_T) = \tau^*$ at the population dynamic equilibrium. We calculate τ^* by setting $\frac{N_{T+1}}{N_T} = 1$ in Equation (1):

$$\tau^* = \frac{1}{(FG^B)}.$$

If $\tau_1(N_T) > \tau^*$, plants outlive the species' break-even time, making LRS >1 and causing abundance to increase, whereas if $\tau_1(N_T) < \tau^*$, the species' population decreases. This formula turns out to be the same in the multispecies problem described in the next section, where the break-even time is species-specific: $\tau_i^* = \frac{1}{F_i G_i^B}$.

We now re-write Equation (1) in terms of the break-even time τ^* as

$$\frac{N_{T+1}}{N_T} = \frac{\tau_1(N_T)}{\tau^*} \quad (2)$$

which reveals the direct relationship between growing season length and population growth. The biomass conversion to seed, F , and within season biomass growth rate, G^B , remain important determinants of between year population growth, but their effects operate by changing a species' break-even time τ^* . A species producing more seeds per unit biomass (higher F) can replace itself with less biomass production over the year and can thus sustain a population while stopping growth earlier in the season (have a lower τ^*).

Water availability affects population growth across years via its effect on the length of a species' growing season $\tau_1(N_T)$, which is itself a function of the depletion of soil water. Putting aside for the moment the details of the depletion process, a species can put on biomass as long as the soil water availability exceeds its critical water threshold. This leads naturally to a condition for positive growth when rare. A species can invade an empty system from low density provided the amount of water available at its break-even time, $W(\tau_1^*)$, is greater than its critical soil water content, W^* , as this implies it is able to outlive its break-even time. Since a species has negligible effect on soil water content at low density, this is true when:

$$W(\tau_1^*) > W^*, \quad (3)$$

where $W(\tau)$ where describes pre-invasion, within-season water availability as a function of, and $W(\tau_1^*)$ gives the value of this function at the species' break-even time. We denote the amount of water available at the beginning of the growing season W_0 , and in a system with no plants, soil water stays at this level through the entire season $W(\tau) = W_0$. What follows is a very simple graphical method for determining whether a species can invade the system with no other competitors present. First, we plot water availability through the year, $W(\tau) = W_0$ on a plot of W versus τ , and then add a point corresponding to the species' critical water content, W^* , and break-even time, τ_1^* , (Figure 1a). If that point lies above the water availability line, $W^* > W_0$, the water supplied is less than the species' soil water threshold and the population goes extinct

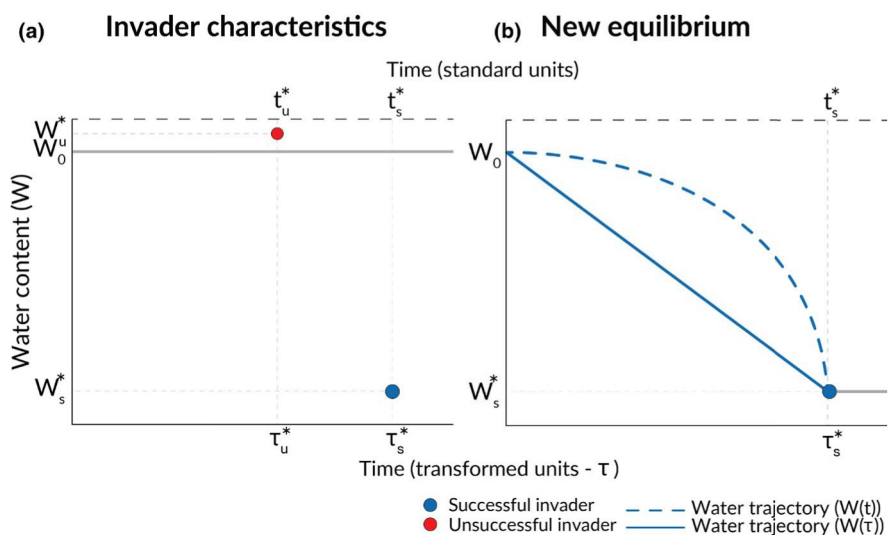


FIGURE 1 Graphical method for determining invasion success for a single-species system. In Panel A, the grey line denotes the pre-invasion water trajectory, $W(\tau)$, which remains flat at the initial water content, W_0 , due to the lack of transpiration, evaporation or precipitation. The red dot describes the characteristics of an unsuccessful invading species with break-even time τ_u^* (τ_u^* in standard units) and

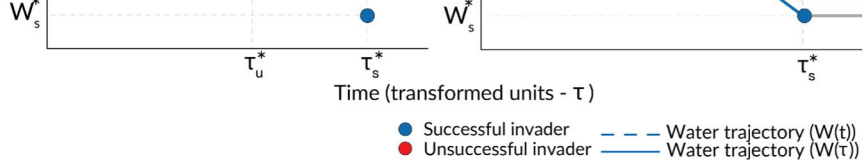


FIGURE 1 Graphical method for determining invasion success for a single-species system. In Panel A, the grey line denotes the pre-invasion water trajectory, $W(\tau)$, which remains flat at the initial water content, W_0 , due to the lack of transpiration, evaporation or precipitation. The red dot describes the characteristics of an unsuccessful invading species with break-even time τ_u^* (t_u^* in standard units) and critical soil water content W_u^* . The invader is unsuccessful because its critical soil water content is greater than the initial water content and therefore cannot increase in biomass. The blue dot denotes the characteristics of a successful invading species with break-even time τ_s^* (t_s^* in standard units) and critical soil water content W_s^* . The subscript s denotes a successful invader, while the subscript u denotes an unsuccessful invader. In Panel B, the characteristics of the successful invader are again described by the blue dot. In the resulting single-species equilibrium, the solid blue line describes the water drawdown trajectory, $W(\tau)$, from the initial water content to the invading species' critical soil water content at $\tau = \tau^*$ in transformed time units. The dashed blue line shows the water drawdown trajectory in standard time units, $W(t)$.

(Figure 1a). If the point lies below the water availability line, then $W^* < W_0$, more water is supplied than the species' threshold water level, and the species will successfully invade (Figure 1a).

To determine a species' population growth rate ($\frac{N_{T+1}}{N_T}$) and growing season length ($\tau_1(N_T)$) away from equilibrium, as well as the resulting soil water trajectory, $W(\tau)$, we must model water depletion. The water available at the end of the species' growing season, or equivalently, that species' shut-off point, W^* , equals the water available at the beginning of the growing season, W_0 , minus the water consumed by the species from the beginning of the season to the end, $\tau_1(N_T)$. More formally:

$$W^* = W_0 - E \int_0^{\tau_1(N_T)} \Lambda(\tau) \frac{dt}{d\tau} d\tau, \quad (4)$$

where E is the transpiration rate per unit leaf area (Box 1) and $\Lambda(\tau)$ is the total leaf area at time τ (see Appendix 2.3 for the functional form of $\Lambda(\tau)$). Water consumption is, thus, a time-integrated function of the leaf area of the population from the start of the season to the time it stops growing. Given that W^* and W_0 are fixed parameters of the species and system, growing season length is calculated by integrating the right hand side of Equation (4) and solving for $\tau_1(N_T)$ (see Appendices 3.1 and 5 for the solutions). This value, when placed into Equation (2), gives the population growth rate.

Integrating Equation (4) and subsequent algebra (Appendix 3.4) produces an expression for the within-season water availability, a piecewise linear function of τ . Specifically, when $T > 0$:

$$W(\tau) = \begin{cases} W_0 - \left(\frac{W^* - W_0}{\tau_1^*} \right) \tau & 0 \leq \tau < \tau_1^* \\ W^* & \tau \geq \tau_1^* \end{cases}. \quad (5)$$

This means that in all years ($\tau > 0$), within-season water availability, $W(\tau)$, follows a straight line on a plot of τ versus W from $\tau = 0$, $W = W_0$ to ($\tau = \tau_1^*$, $W = W^*$) as shown in Figure 1b, which also implies that the species reaches its population dynamic equilibrium in a single year (see Appendix 3.4).

A model of two species

The mechanisms governing competition and coexistence of two species can be extended from the rules for a single species to invade. We now label the species using the subscripts 1 and 2 such that species 1 finishes its growing season before species 2 (i.e., $W_1^* > W_2^*$). Coexistence can be predicted from just the break-even times and critical water values of the two competitors. To show this, we take a mutual invasion approach to coexistence, first considering whether an early species can invade a late-season competitor. This can be determined by applying the graphical method developed in the single-species case. In fact, identical to the water drawdown in the single-species model (Figure 1b), is the pre-invasion water drawdown, $W(\tau)$, by the late season resident species at equilibrium (solid blue line in Figure 2a). Here, $W(\tau)$ is given by Equation (5) (with subscripts changed to reflect that species 2 is the

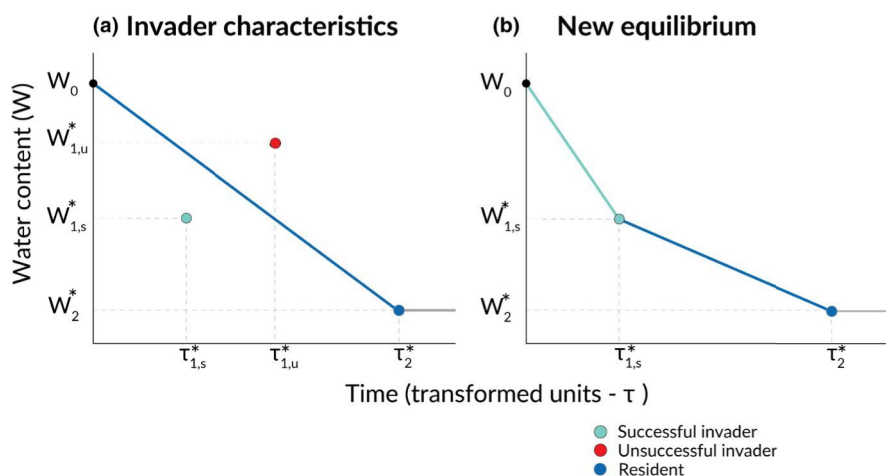


FIGURE 2 Graphical method for determining invasion success in the two-species system. In Panel A, the late-season resident species (species 2) is the same as the invading species from Panel B of Figure 1, with the equilibrium water drawdown trajectory in transformed time units, $W(\tau)$, shown by the same solid blue line. The characteristics of an unsuccessful early-season invading species (species 1) are denoted by the red dot. Because the invading species' characteristics lie above the water drawdown trajectory, the resident species depletes water too quickly for the invader to grow to its break-even time. The characteristics of a successful invading species are given by the light blue dot in Panel A. In Panel B, the characteristics of the successful invading species are again shown. At the resulting two-species equilibrium, the water drawdown trajectory, $W(\tau)$, is given by both the light and dark blue lines. In the first phase, in which both species grow, the water decreases steeply to reach species 1's critical soil water content at its break-even time. Then, after species 1 converts to seed, the water is withdrawn by species 2 alone until its critical soil water content and break-even time are reached.

resident). The question for invasibility is whether the resident species consumes water too fast for the invading species to reach its break-even time. To answer this, we determine whether $W(\tau_1^*) > W_1^*$ by plotting the point corresponding to the invader's critical water content and break-even time ($W = W_1^*$, $\tau = \tau_1^*$). If this point lies above the line corresponding to the water dynamics when the resident is at equilibrium, $W(\tau)$, the invader's critical water value, W_1^* , is reached (along the resident's line) before its break-even time τ_1^* , and thus the invasion will be unsuccessful (Figure 2a). If, instead, the point lies below the water-drawdown line, the system with just the resident species reaches the invader's critical water value after the invader's break-even time, and the invasion will be successful (Figure 2a).

In contrast to the questionable invasion of an earlier season competitor, a late-season species can always invade an early-season resident species. This is because a late-season species (species 2) has unrivalled access to water after species 1 stops growing, and because we have assumed for simplicity that the only way the soil can lose water is through transpiration. Thus, an infinitesimal invading population of species 2 will grow forever on the finite water available after species 1 has stopped transpiring. It is straightforward to eliminate this unrealistic dynamic by adding evaporative water loss. However, because the results are qualitatively similar, but more analytically cumbersome, we continue to assume a lack of evaporation while recognising that this does not fully capture the true resource dynamics of the late season (Appendix 9.1).

Given that a late-season species can always invade an early-season resident, the invasion condition for the early-season species, $W(\tau_1^*) > W_1^*$, is sufficient for mutual invasion. Substituting Equation (5) into this condition and following algebra, we find:

$$\frac{W_0^* - W_1^*}{\tau_1^*} > \frac{W_0^* - W_2^*}{\tau_2^*}, \quad (6)$$

(see Appendix 5.1 for derivation). This implies that in order to coexist, the earlier species must be able to consume water faster over the time it takes to produce one new individual per capita than the later species consumes water over the time it takes to produce one new individual per capita. If this condition is met, species 1 is more than compensated for its reduced access to water by a growth rate advantage (shorter τ_1^*) relative to species 2. If species 1 is not a sufficiently fast grower during its shorter period of water access, it will be excluded.

If a species is successful in invading the resident, the population density of the invading species will increase,

it now has three phases. In the first phase, both species grow and consume water until species 1's critical water content, W_1^* , is reached. Then, in the second phase, only the late-season species continues growing and consuming water until its critical water content, W_2^* , is reached. Finally, in the third phase, water availability remains at W_2^* until the season ends. At equilibrium, $W(\tau)$ for a two-species system is given by:

$$W(\tau) = \begin{cases} W_0 - \left(\frac{W_1^* - W_0}{\tau_1^*} \right) \tau & 0 \leq \tau < \tau_1^* \\ W_1^* - \left(\frac{W_1^* - W_2^*}{\tau_2^* - \tau_1^*} \right) (\tau - \tau_1^*) & \tau_1^* \leq \tau < \tau_2^* \\ W_2^* & \tau \geq \tau_2^* \end{cases} \quad (7)$$

Thereby at equilibrium, water availability follows a straight line on a plot of τ versus W first from $(\tau = 0, W = W_0)$ to $(\tau = \tau_1^*, W = W_1^*)$, and then from $(\tau = \tau_1^*, W = W_1^*)$ to $(\tau = \tau_2^*, W = W_2^*)$ (Figure 2b).

A model of Q species

We now extend the two species result to an arbitrary number of species, Q , and label species $i = 1, \dots, Q$, such that species 1 again has the shortest growing season length, while species Q has the longest (i.e. $W_1 > W_2, \dots, W_Q$). We again develop a graphical methodology for determining invasion success for systems with more than two species. Figure 3 illustrates this technique for a two-species resident community (the same one from Figure 2, Panel B) and single invader species with an intermediate critical water threshold. Such an invasion can be successful in a two-species resident community provided the point corresponding to its critical water threshold and break-even time lies below the water drawdown trajectory, $W(\tau)$, for the resident community. This indicates that the resident community consumes water slowly enough for the invader to reach its break-even time before the water level drops to its critical water threshold. (Figure 3).

At equilibrium, water drawdown in a Q -species system is again given by a piecewise linear function of τ :

$$W(\tau) = \begin{cases} W_0 - \left(\frac{\Delta W_1^*}{\Delta \tau_1^*} \right) \tau & 0 < \tau < \tau_1^* \\ W_{i-1}^* - \left(\frac{\Delta W_i^*}{\Delta \tau_i^*} \right) (\tau - \tau_{i-1}^*) & \tau_{i-1}^* \leq \tau < \tau_i^*, 1 < i < Q \\ W_Q^* & \tau \geq \tau_Q^* \end{cases} \quad (8)$$



new individual per capita than the later species consumes water over the time it takes to produce one new individual per capita. If this condition is met, species 1 is more than compensated for its reduced access to water by a growth rate advantage (shorter τ_1^*) relative to species 2. If species 1 is not a sufficiently fast grower during its shorter period of water access, it will be excluded.

If a species is successful in invading the resident, the population density of the invading species will increase, and that of the resident species will decrease until both reach their new, two-species equilibrium population densities (Appendix 3.3). As with the single-species model, for all years $T > 0$ the within-season water availability, $W(\tau)$, is a piecewise linear function of τ , though

tem is again given by a piecewise linear function of τ :

$$W(\tau) = \begin{cases} W_0 - \left(\frac{\Delta W_1^*}{\Delta \tau_1^*} \right) \tau & 0 < \tau < \tau_1^* \\ W_{i-1}^* - \left(\frac{\Delta W_i^*}{\Delta \tau_i^*} \right) (\tau - \tau_{i-1}^*) & \tau_{i-1}^* \leq \tau < \tau_i^*, 1 < i < Q \\ W_Q^* & \tau \geq \tau_Q^* \end{cases} \quad (8)$$

where $\Delta W_i^* = W_{i-1}^* - W_i^*$, $\Delta \tau_i^* = \tau_i^* - \tau_{i-1}^*$ and $\tau_0 = 0$. The growing season is thereby divided into $Q + 1$ periods, each defined by the number of species left growing and consuming water. Species drop out of the system sequentially as their critical water contents are reached until none remain.



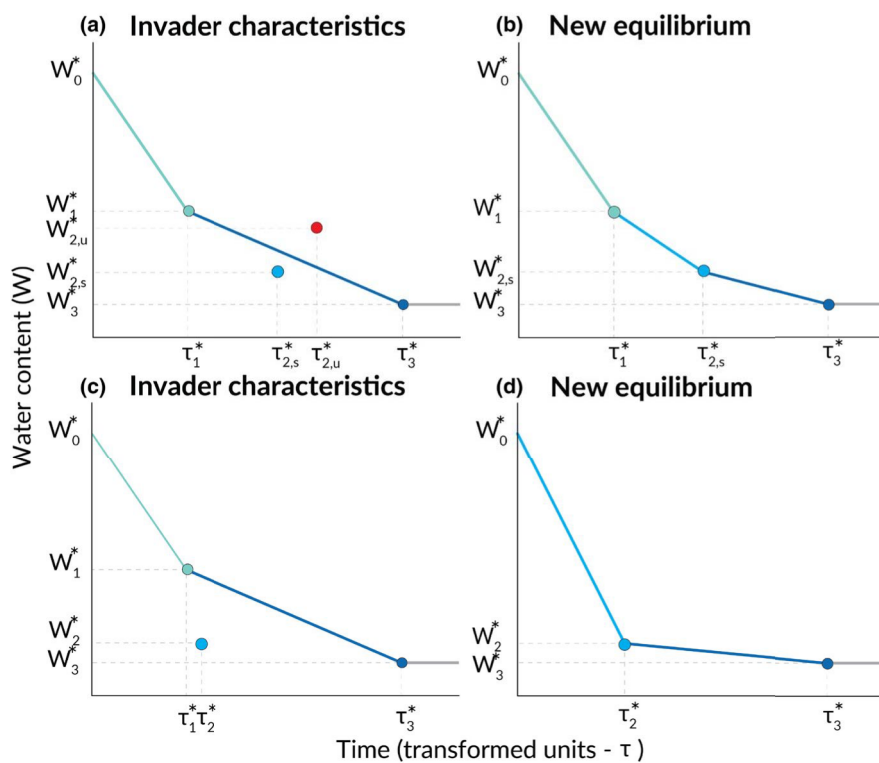


FIGURE 3 Graphical method for determining invasion success – three-species system. In Panel A, the resident two-species community (species 1 and 3) is the same as that from Panel B of Figure 2, with the equilibrium water drawdown trajectory, $W(\tau)$, shown by the same solid blue lines. The characteristics of an unsuccessful intermediate-phenology invading species (species 2) are again denoted by the red dot. Because the invading species' characteristics lie above the water drawdown trajectory, the resident community consumes water too quickly for the invader to grow to its break-even time. The characteristics of a successful invading species are given by the blue dot of intermediate hue in Panel A. In Panel B, the characteristics of this successful invading species are again displayed. At the resulting three-species equilibrium, the water drawdown trajectory is given by three solid blue lines. In the first phase, in which all three species grow, the water decreases steeply to reach species 1's critical soil water content at its break-even time. Then, after species 1 converts to seed, the water is withdrawn by species 2 and 3 until species 2's critical soil water content and break-even time are reached. Finally, species 3 withdraws water alone until its critical soil water content and break-even time are reached. In Panel C, the characteristics of a successful invader are again shown by the blue dot of intermediate hue. This species will invade successfully and subsequently cause species 1 to be excluded, as the resulting community will withdraw water too quickly for species 1 to grow to its break-even time. Panel D shows the resulting two-species equilibrium, in which only species 2 and species 3 persist.

Using the invasion condition, $W(\tau_i^*) > W_i^*$, and Equation (8), we find that mutual invasion in a Q -species system requires that the following expression (see Appendix 4) is satisfied for all adjacent pairs of species, once ordered according to W_i^* :

$$\frac{\Delta W_i^*}{\Delta \tau_i^*} > \frac{\Delta W_{i+1}^*}{\Delta \tau_{i+1}^*}. \quad (9)$$

This condition requires that later-phenology species cannot consume water at a rate which prevents earlier phenology species from reaching their break-even times at low density.

Importantly, a species which successfully invades a Q -species resident community can cause earlier residents to be excluded (a later resident always persists following the reasoning in the two-species section above). Returning to the case of a species with intermediate critical water content invading a two-species resident system: exclusion

of the earlier resident will occur if the invading species has a faster water consumption rate at its single-species equilibrium than the earlier resident (i.e. if Equation (9) is not satisfied for $i = 1$; Figure 3b). In this case, the invading species has a greater biomass growth advantage (lower τ_i^*) in proportion to its water access than the resident does and will, therefore, consume water fast enough that the resident with a higher critical water threshold can no longer reach its break-even time at low density (Figure 3c).

In a system of Q competing species, the subset which eventually coexists can be determined using a simple graphical algorithm. To start, we plot the minimum soil water content, W_i^* , and break-even time, τ_i^* , for each of the Q species as we have done in the single-, two- and three-species cases (Figure 4a). Next, we draw a line from the point corresponding to the initial water content ($W = W_0$, $\tau = 0$) to the species' point for which the resulting line has the steepest negative slope. Then, we draw a line from that species' point to another species'

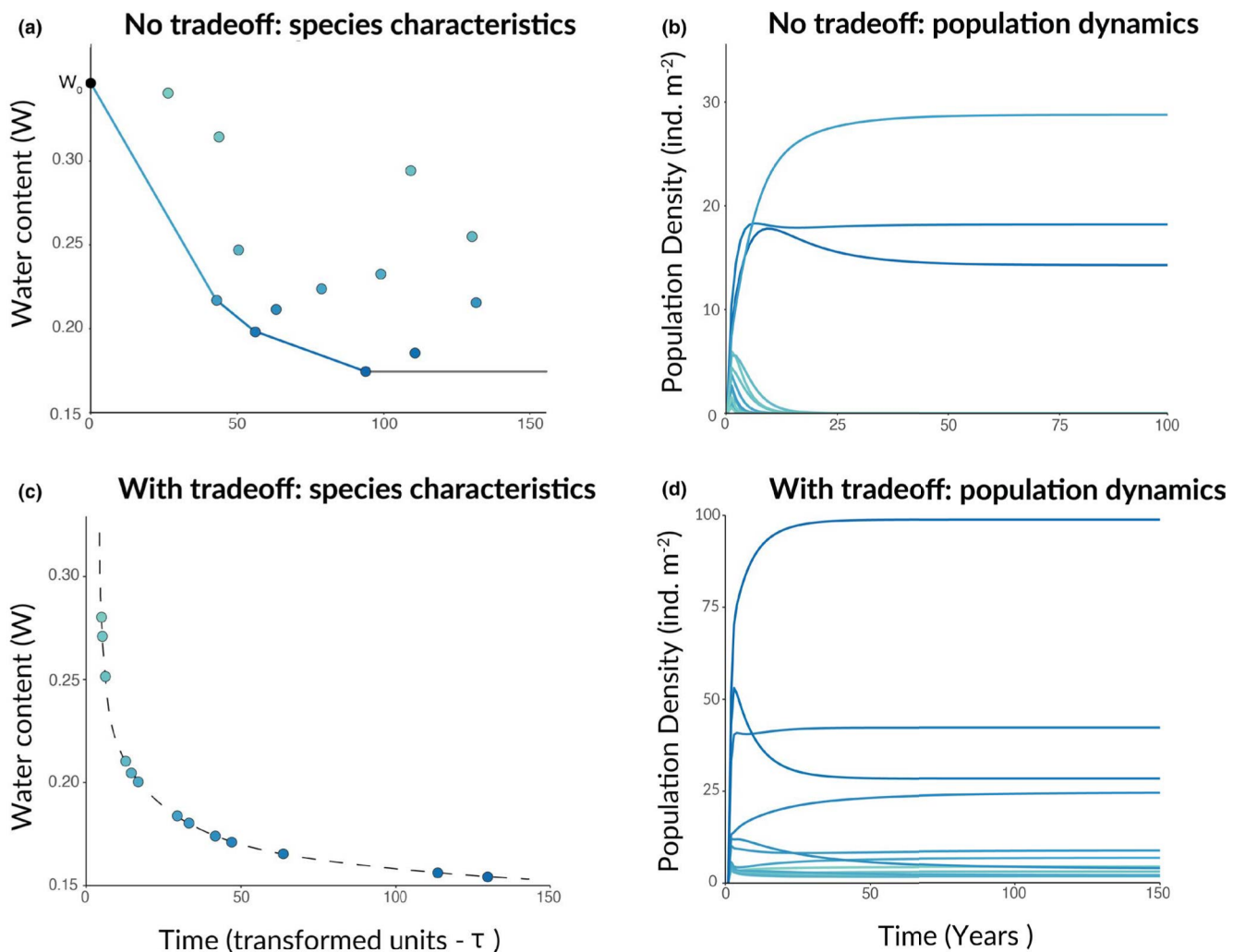


FIGURE 4 Coexistence outcomes in large species assemblages as a function of an interspecific trade-off. Panel A shows an assemblage of 13 species with randomly selected critical soil water contents and break-even times. The graphical method is used to determine the subset of these species which will persist in time. The characteristics of these three species are connected by solid lines which denote the water drawdown trajectory at the resulting equilibrium. Panel B displays the population dynamics in time for the 13 species assemblage, with the three coexisting species forming an equilibrium and the rest collapsing to zero. Panel C shows an assemblage of 13 species with characteristics chosen according to a trade-off curve which satisfies the coexistence conditions. Panel D displays the population dynamics for these species over time, with all species converging to positive equilibrium densities.

point, again minimising the slope of the resulting line. We continue connecting the dots from the left to the right until we cannot draw a new line that is negative in slope. Following the condition in Equation (9), all of the connected species will coexist, the rest will be excluded. The set of species which persist in equilibrium is, thus, given by the lower, convex hull of the point cloud that results from plotting each species' minimum water content and break-even time, as well as the point corresponding to the start of the season ($W = W_0, \tau = 0$).

An interesting consequence of the coexistence in

species pool prior to assembly. This emphasises that one cannot infer the existence of a physiological trade-off from the traits of coexisting species.

If instead of forming a point cloud like in Figure 4a, species adhere to a strict decreasing and concave-up trade-off like that in Figure 4c, then every species in a set that has τ_i^* greater than a threshold value (see Appendix 4) will coexist with one another no matter how many are placed in competition. This is again because early-season species are more than compensated for their shortened growing seasons by increased growth rates,



right until we cannot draw a new line that is negative in slope. Following the condition in Equation (9), all of the connected species will coexist, the rest will be excluded. The set of species which persist in equilibrium is, thus, given by the lower, convex hull of the point cloud that results from plotting each species' minimum water content and break-even time, as well as the point corresponding to the start of the season ($W = W_0, \tau = 0$).

An interesting consequence of the coexistence in Figure 4a is that after community assembly all coexisting species will appear to exhibit a trade-off, in that the early-season species will have both faster growth and a higher minimum water threshold than the late-season species, even if no physiological trade-off exists in the

from the traits of coexisting species.

If instead of forming a point cloud like in Figure 4a, species adhere to a strict decreasing and concave-up trade-off like that in Figure 4c, then every species in a set that has τ_i^* greater than a threshold value (see Appendix 4) will coexist with one another no matter how many are placed in competition. This is again because early-season species are more than compensated for their shortened growing seasons by increased growth rates, allowing them to reach their break-even time before their late-season competitors reduce soil water content below their critical value.

Indeed, there are physiological reasons to expect the very trade-off allowing coexistence. First, note that



satisfying the mutual invasion condition in Equation (9) requires a trade-off between a species' ability to tolerate low water (its W_i^*), and the speed at which it accumulates biomass (which shortens τ_i^*). More precisely, for all species to coexist, the functional relationship between species' critical water threshold and break-even time must be negative (higher water thresholds mean faster break-even times), and concave up (progressively longer break-even times mean lesser advantages in critical water threshold) (Figure 4). Finally, the trade-off curve must be restricted to species with minimum water thresholds below W_0 because any species with $W^* > W_0$ would go extinct even without the presence of a competitor.

Notably, when allocational constraints are incorporated into the physiological model of plant growth under water limitation, a trade-off curve that is both negative and concave-up emerges. That model, presented in Appendix 1 and 4.2, predicts that species should be perfectly ordered such that as a species' growth rate, G_i^B , increases (which decreases its τ_i^*), its threshold soil water content necessary for continued growth, W_i^* , also increases (Box 1, Appendix 1.1). The reason for this relationship is that plant traits that allow transpiration at low levels of soil moisture, such as dense stem tissue that resists embolism (Rosner, 2017), require photosynthate that could have been used for productive tissues like leaves. Allocating photosynthate to embolism-resistant structures then slows the rate of biomass growth. The positive correlation between G_i^B and W_i^* , together with the monotonic drying of the soil after the winter rains, implies a trade-off between biomass growth rate and growing season length, τ_i^* , that has negative slope. As we explain more fully in Appendix 4.2, the trade-off is also likely to have a concave-up shape because the growth cost to reduce one's critical soil water content increases in magnitude for lower values of W^* . These accelerating growth costs mean that as W^* decreases, the corresponding changes in break-even time (the inverse of growth) also increase (Appendix 4.2).

The Appendices present several additional analyses that could not be included in the manuscript but are worth mentioning here. First, we prove that a Q -species equilibrium, if it exists, is unique (Appendix 3.3). We show that for any combination of species, invasion when rare implies the existence of a positive equilibrium (Appendix 4.1). Moreover, we derive a time-dependent solution of species abundances in a two-species system and prove that any two-species positive equilibrium is globally stable (Appendix 6). We also prove that in a Q -species system any positive equilibrium is locally stable (Appendix 7). Last, we show that the trade-offs which imply the existence of a stable equilibrium in the population dynamics correspond precisely to a model of plant physiology (Appendix 4.2), suggesting that our coexistence criteria may be generally satisfied for annual plant communities whose physiology is accurately described by our model.

EMPIRICAL SYSTEM AND QUALITATIVE MODEL VALIDATION

Our prior empirical work with phenologically distinct annual plants at the University of California, Sedgwick Natural Reserve in northern Santa Barbara County, California, USA, (Alexander & Levine, 2019; Godoy & Levine, 2014) has identified several qualitative patterns that our model should be able to reproduce. First, a trade-off should exist such that species that stop growing earlier in the season grow faster than later taxa over their period of overlap. Second, competitive exclusion is always suffered by the species with the earlier phenology; the later species persists due to its access to late-season water. Third, earlier phenology of a late-season species increases its competitive effect on earlier taxa and reduces their invasion growth rate.

First, we evaluate the trade-off. Godoy and Levine (2014) quantified the biomass accumulation of three non-native plant species in the system, *Bromus madritensis*, *Centaurea melitensis* and *Lactuca serriola*, as well as the date they stopped growing. These taxa were in fact chosen for study because they stop growing at different times of the year. Not only do these species exhibit something close to power-law growth, as assumed here, but each species is the most rapid accumulator of biomass during their period of overlap with later competitors (Figure 5a). This result, of course, is consistent with trade-offs that underlie coexistence in our model. Assemblages of early, middle and late *native* species in the same study did not show such trade-offs, but it is unclear whether these taxa would coexist with one another at the local scale of the study plots (Kraft et al., 2015).

Second, we evaluate the pattern of competitive exclusion. Godoy and Levine (2014) parameterised Lotka–Volterra type population dynamic models of competition between each native community (early, middle and late) and each non-native species (Figure 5b). These models predicted competitive exclusion for eight of nine pairs. Importantly, regardless of the species' native or non-native status, it was always the earlier species that was excluded. This qualitative pattern is consistent with results from our model, where exclusion always eliminates the earlier species because the later competitor has unique access to water unconsumed by its earlier counterpart.

Third, we evaluate our model's ability to predict the competitive effect of a later taxa as a function of its phenology. Alexander and Levine (2018) explored how differences in phenology between populations of a late-season invader, *Lactuca serriola*, affected its suppression of earlier phenology native plants. Results showed that earlier *Lactuca* populations exerted greater per capita competitive effects on the per germinant fecundity of native plants (Figure 5b), which reduced their



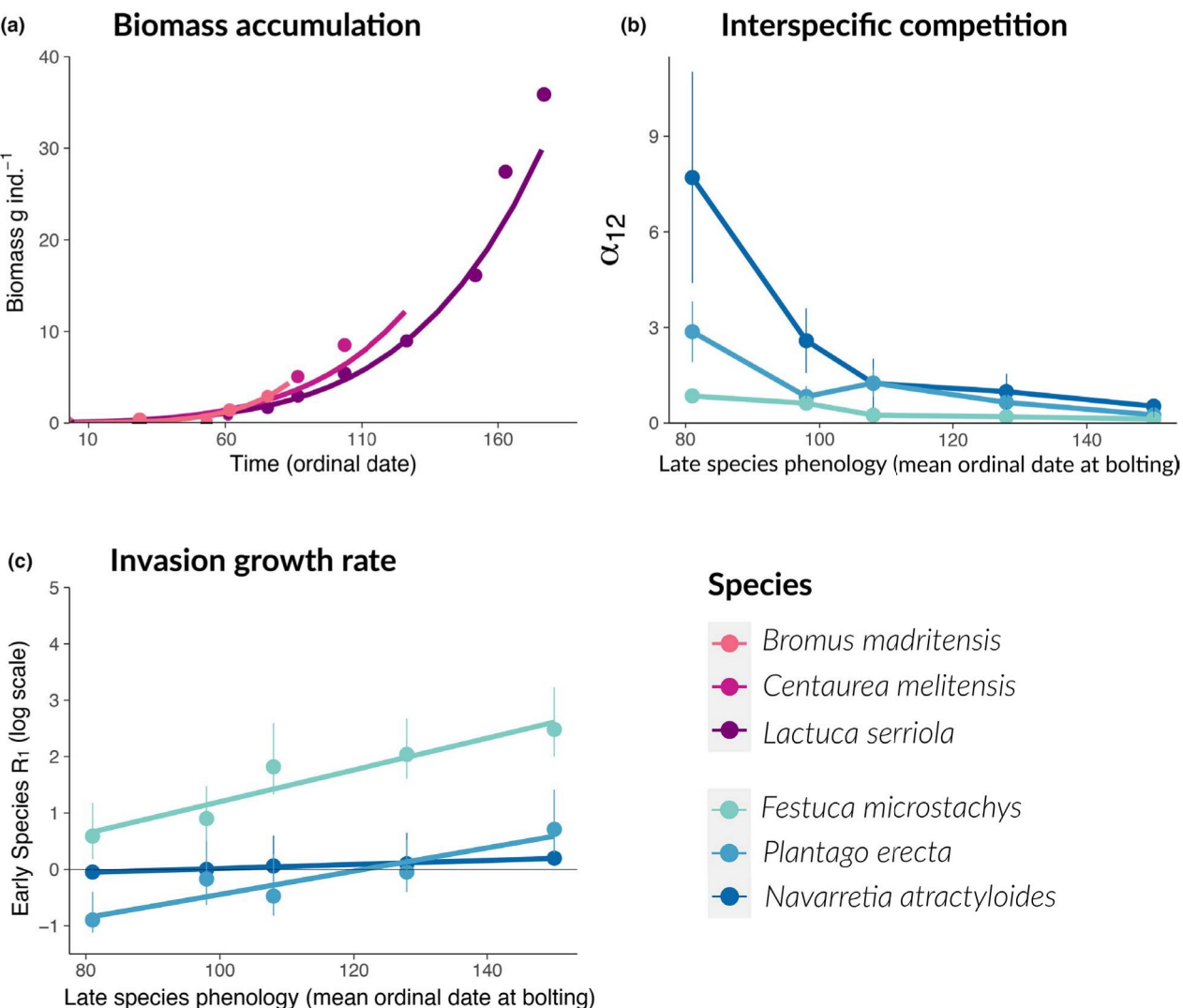


FIGURE 5 Patterns from empirical studies of phenology and coexistence in California Mediterranean annual plant communities and predicted patterns from theoretical model. Panel A shows the change in biomass over time for individuals of three species of differing phenology (*B. madritensis*, *C. melitensis* and *L. serriola*). Empirical data are denoted by the points, coloured according to species phenology. Power-law fits to the data are shown as solid lines. Panel B shows the per capita competitive effect of a late season species, *L. serriola*, on three resident species of varying phenology (*P. erecta*; *F. microstachys* and *N. atractyloides*) (α_{12}) as a function of late-season species phenology, expressed as the mean ordinal date at bolting. Panel C shows the log low-density growth rate (R_1) of three resident species of varying phenology (*P. erecta*; *F. microstachys* and *N. atractyloides*) as a function of the phenology of a late season species, *L. serriola*. In panels B and C, error bars describe the variation around mean values (points). In panel C linear regressions are overlaid to show the trend.

projected invasion growth rates (Figure 5c). Both of these results also emerge from our model. To see how, first note that the per capita competitive effect of a later competitor on the growth of an earlier one is calculated as $\frac{G_{late}^{R-1}}{G_{early}^R}$ (Appendix 3.6). From this expression, it is clear that a higher biomass growth rate of the later competitor will increase its competitive effect. A higher biomass growth rate of earlier *Lactuca* would be expected if the species-level trade-off between phenology

DISCUSSION

In this paper, we introduced a mechanistic model of phenologically structured water competition between annual plants. Our model is built on a foundation of realistic ecohydrology, plant physiology and allometry, can readily replicate and explain empirically observed patterns, and provides several fundamental insights into the interactions allowing for the coexistence of annual

projected invasion growth rates (Figure 5c). Both of these results also emerge from our model. To see how, first note that the per capita competitive effect of a later competitor on the growth of an earlier one is calculated as $\frac{G_{late}^{R-1}}{G_{early}^R}$ (Appendix 3.6). From this expression, it is clear that a higher biomass growth rate of the later competitor will increase its competitive effect. A higher biomass growth rate of earlier *Lactuca* would be expected if the species-level trade-off between phenology and biomass growth rate (Figure 5a) holds within species. This same mechanism in our model also causes an earlier species invasion growth rate to decrease as the later species phenology moves up in time, matching the empirical data (Figure 5c).

DISCUSSION

In this paper, we introduced a mechanistic model of phenologically structured water competition between annual plants. Our model is built on a foundation of realistic ecohydrology, plant physiology and allometry, can readily replicate and explain empirically observed patterns, and provides several fundamental insights into the interactions allowing for the coexistence of annual plants competing for water in Mediterranean climates. In the model, phenological differentiation arises naturally through interspecific variation in the critical soil water threshold and a transpiration-driven, monotonic decrease in water content through the growing season.

When accompanied by a trade-off in growth rate, the resulting phenological nesting of competitors can maintain unlimited species diversity under simple but realistic assumptions.

The mechanism of coexistence

Pairwise coexistence occurs in the model because an earlier competitor with a higher water threshold, if it grows fast enough, achieves the biomass necessary for positive population growth before all its later competitors deplete the water to its critical value. Meanwhile, a later species always persists with earlier, more water-demanding taxa due to its ability to grow during the period after these earlier taxa senesce. Moreover, this extends to any number of earlier and later competitors. In a Q-species system, the growing season is subdivided into periods with stepwise decreases in diversity as a result of interspecific differences in critical soil water content and a monotonically decreasing soil water pool. When this pattern is paired with a relationship between species' break-even times and critical water thresholds that is both negatively sloped and concave-up (Figure 4, Panels C and D), each species is the dominant competitor for water in exactly one time period – the one in which they are the earliest phenology species still growing. Under such conditions, each species is able to grow fast enough to achieve positive population growth before its competitors reduce water to its critical value.

Unlimited coexistence is only possible when species' traits are perfectly constrained to follow a negatively sloped, concave-up trade-off. However, whether or not such a relationship between break-even time and critical water threshold exists, any set of coexisting species will appear to exhibit a trade-off of this form simply because it is a requirement for coexistence (Figure 4a). Species that fall above the trade-off curve will have been excluded. This illustrates how the presence of an apparent trade-off in traits among co-occurring species need not imply the existence of a true allocational trade-off related to constraints on how plants are built. To determine whether such a trade-off exists, one must examine the underlying ecophysiological relationships between traits in a broader pool of species, including those that coexist and those that exclude one another.

A key element of annual plant life history is in part responsible for the high degree of coexistence possible in the model: the invulnerability of the seed stage to competition. Species escape the negative effects of the unfavourable environment created by their competitors by converting their biomass to dormant seeds when they reach their critical water threshold. Though species cannot grow during the portion of the season in which soil water content is below their critical threshold, they do not suffer the negative consequences of competition-induced water limitation during that period. And, of

course, the later competitor suffers nothing from the dormant seeds.

Competition for time

When competitors in the model deplete soil water, they alter the length of each species' growing season, which, in turn, determines their invasion success, equilibrium abundance and population growth rate. Thus, by differentially depleting a shared water resource, species are effectively competing for time. Competition for time dynamics have also emerged in other physiologically grounded resource-competition models. For example, Detto et al. (2021) develop a model of light competition in both forest and annual plant systems in which species grow unfettered by neighbours until they are overtapped by taller competitors. As in our model, the ability of a species to invade a system of competitors is a function of the amount of time it has to grow before being overtapped. Although species in Detto et al. (2021)'s model ostensibly compete for light, they in fact compete by shortening the growing season lengths of shorter species. Detto et al. (2021) also show unlimited coexistence in their model, and this requires a trade-off between growth duration in the form of overtapping ability and growth rate that is similar to the trade-off required for coexistence in our model. The parallels between these two models suggest that there may be something fundamental about temporal competition and compensating trade-offs that enable many species to coexist.

How simple dynamics emerge from complex physiology

We find it remarkable how the physiological, population dynamic and hydrologic complexity in this model condenses into the simple graphical algorithm illustrated in Figure 4a. As the Appendices make clear, there are many physiological and individual-level parameters that collectively determine the two critical species-specific quantities τ_i^* and W_i^* . All these parameters can be species-specific with the sole exception of the allometric exponent B , which must be common to all species for there to be a single time scale, τ that makes the within-season water dynamics linear. And yet, all of this species-specific complexity reduces to just two critical quantities. One implication of this reduction is that incorporating between-species variation in other functional traits into the model should not reduce the capacity for coexistence, as it will also condense into the two critical species-specific quantities. A second implication is that one should not expect functional trait variation below the level of these two critical quantities to predict coexistence, and this



counters to a large literature that attempts to draw such connections (e.g. Kraft et al., 2015; McGill et al., 2006; Weiher & Keddy, 2001).

The simple, tractable dynamics in the model emerge primarily due to the special, but physiologically derived, scaling between leaf area and biomass. In the model, water availability is a time-integrated function of the transpiration rate, which is itself proportional to a plant's leaf area. Reproduction, however, is simply proportional to a species' end-of-season biomass. Because of the power-law allometric scaling between leaf area and biomass (Appendix 2), leaf area, when integrated, has the same exponent, B , as biomass (Appendix 2.3). Thus, both transpiration and biomass accumulation, and therefore water availability and reproduction, are linear in the same transformed time scale. This allows the simple graphical method for determining coexistence outcomes, the derivation of expressions for the equilibrium abundances and invasion growth rates for systems with an arbitrary number of species and the clear stability properties of the model.

Connection to empirical systems and other coexistence studies

There is substantial evidence that trade-offs between phenology (degree of tolerance to dry soil) and biomass growth rate of the sort required for coexistence in our model are common in natural systems. For example, past empirical studies demonstrate such a relationship in Mediterranean annuals (Angert et al., 2009; Figure 5, Panel A), and other taxa (Ackerly, 2004; de Guzman et al., 2017). As discussed previously, these trade-offs may arise either from underlying physiological constraints or simply as a result of competitive sorting. However, there is reason to expect physiological mechanisms involving variation in stem tissue density (and thus in xylem resistance to embolism) and/or root depth to lead to these trade-offs. For example, correlations between stem-tissue/wood density and resistance to embolism have been widely observed across taxa (Hacke et al., 2001; Rosner, 2017). Similarly, deep roots are more expensive to grow and maintain but allow plants to access water only available late in the season (Schenk & Jackson, 2002). Correlations between rooting depth and phenology have been described extensively in Mediterranean annual systems (Godoy & Levine, 2014; Gulmon et al., 1983; Kraft et al., 2015) and other systems and taxa (for example, Wright & van Schaik, 1994). Indeed, when we incorporated allocational trade-offs between rooting depth/stem-tissue density and

example, Chesson et al., 2001 and Mathias & Chesson, 2013 showed that a trade-off between growing season length and growth rate under drying conditions can serve as a coexistence mechanism in Mediterranean perennial and annual systems. In these studies, phenology is a fixed property of the species and thus operates as a temporal storage effect in the taxonomy of modern coexistence theory (Chesson, 2000). In our model, however, phenology is an emergent function of water availability and the resulting coexistence results from a process that seems more analogous to relative non-linearity. This topic could be further explored with the simulation-based approaches to modern coexistence theory developed by Ellner and colleagues (Ellner et al., 2016, 2019).

In addition, several studies have developed empirically validated models of water competition between deep-rooted tree and shallow-rooted grass species to explore tree-grass coexistence in dry savannahs (Eagleson & Segarra, 1985; Walker et al., 1981; Walter, 1971; Ward et al., 2012). The results of these studies are similar to our own, in that coexistence is possible because species with reduced access to water – the grasses (or early-season annuals in our study), are compensated with greater competitive ability.

Limitations

Our model's tractability results from several key simplifications of nature. The first of these is the approximation of growth as a step function of water availability, under which species' growth rates are unaffected by competition during their growing season (Appendix 1.3). This approximation results in a negligible overestimation of total within-season growth relative to the slightly more continuous function predicted by ecophysiology. Additionally, when we relaxed this assumption in model simulations, we still found high diversity (Appendix 9.3). A second major assumption is a spatial homogeneity in water availability. In nature, water resources are spatially structured, particularly with depth (Gulmon et al., 1983; Seabloom et al., 2003), and plants place roots at different depths. In fact, this variation could provide a mechanistic explanation for the phenological differences in our model, as deeper rooted species are able to access deeper pools of water and therefore persist later into the season. Third, we assume that the growing season is potentially unbounded in time because water is only lost to transpiration, and plants do not experience mortality during their growing season. In the appendix, we analyse models which include abiotic soil water loss and density-independent



are more expensive to grow and maintain but allow plants to access water only available late in the season (Schenk & Jackson, 2002). Correlations between rooting depth and phenology have been described extensively in Mediterranean annual systems (Godoy & Levine, 2014; Gulmon et al., 1983; Kraft et al., 2015) and other systems and taxa (for example, Wright & van Schaik, 1994). Indeed, when we incorporated allocational trade-offs between rooting depth/stem-tissue density and growth rate into the physiological model developed in Appendix 1, we found a trade-off curve that is negative and concave-up, as required for unlimited coexistence.

Several other studies have examined the coexistence dynamics of plants competing for water. For

variation could provide a mechanistic explanation for the phenological differences in our model, as deeper rooted species are able to access deeper pools of water and therefore persist later into the season. Third, we assume that the growing season is potentially unbounded in time because water is only lost to transpiration, and plants do not experience mortality during their growing season. In the appendix, we analyse models which include abiotic soil water loss and density-independent mortality and find that these models still support species assemblages with theoretically unlimited diversity (Appendix 9.1 and 9.2).

Finally, in our model, we assume that initial water availability, W_0 , is consistent across years. In

Mediterranean systems, however, there is considerable interannual variability in rainfall which would translate to variation in W_0 across years (Haston & Michaelsen, 1997; Heady 1977; Schonher & Nicholson, 1988). While we do not explicitly consider such variability in our analysis, it would not qualitatively change the results of this paper. Variation in W_0 could cause early-season species to be competitively excluded. However, though the identity of the earliest species in an assemblage might change, an arbitrary number of species could still coexist.

Future directions

Future work could explore competitive dynamics in systems with more complexity by incorporating explicit variation in rooting depth and by examining plants with more complex life histories than annuals. Many studies have explored the impact of rooting depth on competitive ability and coexistence dynamics in plants (Fargione & Tilman, 2005; Holdo, 2013; Nippert & Knapp, 2007; Ward et al., 2012; Yu & D'Odorico, 2015). However, few incorporate realistic models of abiotic soil water movement, a process with complex (Broadbridge et al., 2017), but potentially important implications for competitive outcomes (Manoli et al., 2017). Future efforts could also explore systems with more complex life cycles than annuals. Though models of perennial species may be intractable, simulations and numerical analyses could be used to explore whether trade-offs between water access and growth rate also allow coexistence in those systems.

Finally, our model generates several empirically testable predictions about the dynamics of water competition in Mediterranean annual plant assemblages. These include (1) plants grow unfettered by competition until reaching a species-specific, minimum water requirement, (2) increased competition reduces a plant's fecundity by shortening its growing season and (3) an interspecific, ecophysiological trade-off between growth rate and minimum water requirement facilitates coexistence. These predictions could be tested by combining pairwise competitive experiments (Godoy & Levine, 2014; Alexander & Levine, 2019), which generate competitive outcomes, with measurements of seasonal biomass accumulation rates and coincident water depletion. Combining such empirical approaches with the type of theory developed here offers the chance to rigorously evaluate some ecophysiological mechanisms underlying plant coexistence in nature.

ACKNOWLEDGEMENTS

We thank members of the Levine and Pacala labs for helpful feedback on earlier versions of the manuscript. We also thank Oscar Godoy for providing the data used to generate Figure 5a and the University of California, Sedgwick Natural Reserve for their continued support. Finally, this

material is based upon work supported by the National Science Foundation Graduate Research Fellowship under Awards #DGE-2039656 and by the National Science Foundation under award #DEB-2022213. Any opinions, findings and conclusions or recommendations expressed in this material are those of the author(s) and do not necessarily reflect the views of the National Science Foundation.

AUTHOR CONTRIBUTION

JIL, JML and SWP conceived of and performed the study, TG contributed to the theoretical modeling. JIL wrote the first draft of the manuscript and all authors contributed substantially to writing and revisions.

PEER REVIEW

The peer review history for this article is available at <https://publons.com/publon/10.1111/ele.13990>.

DATA AVAILABILITY STATEMENT

The data supporting these findings and analysis code have been deposited on Figshare (<https://doi.org/10.6084/m9.figshare.19161611>).

ORCID

Jacob I. Levine  <https://orcid.org/0000-0002-7645-2500>
 Jonathan M. Levine  <https://orcid.org/0000-0003-2857-7904>
 Theo Gibbs  <https://orcid.org/0000-0002-1515-8420>

REFERENCES

Ackerly, D. (2004) Functional strategies of chaparral shrubs in relation to seasonal water deficit and disturbance. *Ecological Monographs*, 74, 25–44.

Alexander, J.M. & Levine, J.M. (2019) Earlier phenology of a nonnative plant increases impacts on native competitors. *Proceedings of the National Academy of Sciences of the United States of America*, 116, 6199–6204.

Anderegg, W.R.L., Klein, T., Bartlett, M., Sack, L., Pellegrini, A.F.A., Choat, B. et al. (2016) Meta-analysis reveals that hydraulic traits explain cross-species patterns of drought-induced tree mortality across the globe. *Proceedings of the National Academy of Sciences of the United States of America*, 113, 5024–5029.

Angert, A.L., Huxman, T.E., Chesson, P. & Venable, D.L. (2009) Functional tradeoffs determine species coexistence via the storage effect. *Proceedings of the National Academy of Sciences*, 106, 11641–11645.

Ball, J.T., Woodrow, I.E. & Berry, J.A. (1987) A model predicting stomatal conductance and its contribution to the control of photosynthesis under different environmental conditions. *Progress in Photosynthesis Research*, 221–224.

Broadbridge, P., Daly, E. & Goard, J. (2017) Exact solutions of the Richards equation with nonlinear plant-root extraction. *Water Resources Research*, 53, 9679–9691.

Chesson, P. (2000) Mechanisms of maintenance of species diversity. *Annual Review of Ecology and Systematics*, 31, 343–366.

Chesson, P., Pacala, S. & Neuhauser, C. (2001) Environmental niches and ecosystem functioning. In *The functional consequences of biodiversity*. 10, Princeton: Princeton University Press, pp. 213–245.

Craine, J.M. & Dybzinski, R. (2013) Mechanisms of plant competition for nutrients, water and light. *Functional Ecology*, 27, 833–840.



Craine, J.M., Wolkovich, E.M., Gene Towne, E. & Kembel, S.W. (2012) Flowering phenology as a functional trait in a tallgrass prairie. *New Phytologist*, 193, 673–682.

Daly, E., Porporato, A. & Rodriguez-Iturbe, I. (2004) Coupled dynamics of photosynthesis, transpiration, and soil water balance. Part I: Upscaling from hourly to daily level. *Journal of Hydrometeorology*, 5, 546–558.

de Guzman, M.E., Santiago, L.S., Schnitzer, S.A. & Alvarez-Cansino, L. (2017) Trade-offs between water transport capacity and drought resistance in neotropical canopy liana and tree species. *Tree Physiology*, 37, 1404–1414.

Dettman, M., Levine, J.M. & Pacala, S.W. (2021) Maintenance of high diversity in mechanistic forest dynamics models of competition for light. *Ecological Monographs*, Available at: <https://par.nsf.gov/biblio/10293704> Last accessed 30 September 2021

Eagleson, P.S. & Segarra, R.I. (1985) Water-limited equilibrium of savanna vegetation systems. *Water Resources Research*, 21, 1483–1493.

Ellner, S.P., Snyder, R.E. & Adler, P.B. (2016) How to quantify the temporal storage effect using simulations instead of math. *Ecology Letters*, 19(11), 1333–1342.

Ellner, S.P., Snyder, R.E., Adler, P.B. & Hooker, G. (2019) An expanded modern coexistence theory for empirical applications. *Ecology Letters*, 22(1), 3–18.

Enquist, B.J., West, G.B., Charnov, E.L. & Brown, J.H. (1999) Allometric scaling of production and life-history variation in vascular plants. *Nature*, 401, 907–911.

Fargione, J. & Tilman, D. (2005) Niche differences in phenology and rooting depth promote coexistence with a dominant C4 bunchgrass. *Oecologia*, 143, 598–606.

Farquhar, G.D. & Sharkey, T.D. (1982) Stomatal conductance and photosynthesis. *Annual Review of Plant Physiology*, 33, 317–345.

Farrar, C.E., Tilman, D., Dybzinski, R., Reich, P.B., Levin, S.A. & Pacala, S.W. (2013) Resource limitation in a competitive context determines complex plant responses to experimental resource additions. *Ecology*, 94, 2505–2517.

Fridley, J.D. (2012) Extended leaf phenology and the autumn niche in deciduous forest invasions. *Nature*, 485, 359–362.

Godoy, O. & Levine, J.M. (2014) Phenology effects on invasion success: Insights from coupling field experiments to coexistence theory. *Ecology*, 95, 726–736.

Goldberg, D. & Novoplansky, A. (2009) On the relative importance of competition in unproductive environments. *Society*, 85, 409–418. Author (s): Deborah Goldberg and Ariel Novoplansky Published by: British Ecological Society Stable URL: <http://www.jstor.org/stable/2960565>

Gulmon, S.L., Chiariello, N.R., Mooney, H.A. & Chu, C.C. (1983) Phenology and resource use in three co-occurring grassland annuals. *Oecologia*, 58(1), 33–42.

Hacke, U.G., Sperry, J.S., Pockman, W.T., Davis, S.D. & McCulloh, K.A. (2001) Trends in wood density and structure are linked to prevention of xylem implosion by negative pressure. *Oecologia*, 126, 457–461.

Haston, L. & Michaelsen, J. (1997) Spatial and temporal variability of Southern California precipitation over the last 400 yr and relationships to atmospheric circulation patterns. *Journal of Climate*, 10(8), 1836–1852.

Heady, H.F. (1977) Valley grassland. In: Barbour, M.G. & Major, J. (Eds.) *Terrestrial vegetation of California*. New York: John Wiley and Sons, pp. 491–514.

Holdo, R.M. (2013) Revisiting the two-layer hypothesis: coexistence of alternative functional rooting strategies in savannas. *PLoS One*, 8, e69625.

Proceedings of the National Academy of Sciences of the United States of America, 112, 797–802.

Leuning, R. (1995) A critical appraisal of a combined stomatal-photosynthesis model for C3 plants. *Plant, Cell & Environment*, 18, 339–355.

Levine, J.M. & HilleRisLambers, J. (2009) The importance of niches for the maintenance of species diversity. *Nature*, 461, 254–257.

Manoli, G., Huang, C.W., Bonetti, S., Domes, J.C., Marani, M. & Katul, G. (2017) Competition for light and water in a coupled soil-plant system. *Advances in Water Resources*, 108, 216–230.

Manzoni, S., Vico, G., Katul, G., Fay, P.A., Polley, W., Palmroth, S. et al. (2011) Optimizing stomatal conductance for maximum carbon gain under water stress: a meta-analysis across plant functional types and climates. *Functional Ecology*, 25, 456–467.

Mathias, A. & Chesson, P. (2013) Coexistence and evolutionary dynamics mediated by seasonal environmental variation in annual plant communities. *Theoretical Population Biology*, 84, 56–71.

McGill, B.J., Enquist, B.J., Weiher, E. & Westoby, M. (2006) Rebuilding community ecology from functional traits. *Trends in Ecology & Evolution*, 21, 178–185.

Nippert, J.B. & Knapp, A.K. (2007) Soil water partitioning contributes to species coexistence in tallgrass prairie. *Oikos*, 116, 1017–1029.

Pilar Fernandez-Illescas, C. & Rodriguez-Iturbe, I. (2003) Hydrologically driven hierarchical competition–colonization models: the impact of interannual climate fluctuations. *Ecological Monographs*, 73(2), 207–222.

Rathcke, B. & Lacey, E.P. (1985) Phenological patterns of terrestrial plants. *Annual Review of Ecology and Systematics*, 16, 179–214.

Rodriguez-Iturbe, I. & Porporato, A. (2007) Ecohydrology of water-controlled ecosystems: soil moisture and plant dynamics.

Rosenzweig, M.L. (1968) Net primary productivity of terrestrial communities: prediction from climatological data. *The American Naturalist*, 102, 67–74.

Rosner, S. (2017) Wood density as a proxy for vulnerability to cavitation: size matters. *Journal of Plant Hydraulics*, 4, e001.

Sala, A., Woodruff, D.R. & Meinzer, F.C. (2012) Carbon dynamics in trees: feast or famine? *Tree Physiology*, 32, 764–775.

Schenk, H.J. & Jackson, R.B. (2002) Rooting depths, lateral root spreads and below-ground/above-ground allometries of plants in water-limited ecosystems. *Journal of Ecology*, 90, 480–494.

Schonher, T. & Nicholson, S.E. (1988) The Relationship between California Rainfall and ENSO Events. *Journal of Climate*, 1258–1269.

Schwinning, S. & Kelly, C.K. (2013) Plant competition, temporal niches and implications for productivity and adaptability to climate change in water-limited environments. *Functional Ecology*, 27, 886–897.

Seabloom, E.W., Harpole, W.S., Reichman, O.J. & Tilman, D. (2003) Invasion, competitive dominance, and resource use by exotic and native California grassland species. *Proceedings of the National Academy of Sciences of the United States of America*, 100, 13384–13389.

Sperry, J.S., Venturas, M.D., Anderegg, W.R.L., Mencuccini, M., Mackay, D.S., Wang, Y. et al. (2016) Predicting stomatal responses to the environment from the optimization of photosynthetic gain and hydraulic cost. *Plant, Cell and Environment*.

Tyree, M.T. & Sperry, J.S. (1989) Cavitation and Embolism. *Water*, 19–38.

Walker, B.H., Ludwig, D., Holling, C.S. & Peterman, R.M. (1981)

120, 457–461.

Haston, L. & Michaelsen, J. (1997) Spatial and temporal variability of Southern California precipitation over the last 400 yr and relationships to atmospheric circulation patterns. *Journal of Climate*, 10(8), 1836–1852.

Heady, H.F. (1977) Valley grassland. In: Barbour, M.G. & Major, J. (Eds.) *Terrestrial vegetation of California*. New York: John Wiley and Sons, pp. 491–514.

Holdo, R.M. (2013) Revisiting the two-layer hypothesis: coexistence of alternative functional rooting strategies in savannas. *PLoS One*, 8, e69625.

Hooper, D.U. & Dukes, J.S. (2010) Functional composition controls invasion success in a California serpentine grassland. *Journal of Ecology*, 98, 764–777.

Kraft, N.J.B., Godoy, O. & Levine, J.M. (2015) Plant functional traits and the multidimensional nature of species coexistence. and native California grassland species. *Proceedings of the National Academy of Sciences of the United States of America*, 100, 13384–13389.

Sperry, J.S., Venturas, M.D., Anderegg, W.R.L., Mencuccini, M., Mackay, D.S., Wang, Y. et al. (2016) Predicting stomatal responses to the environment from the optimization of photosynthetic gain and hydraulic cost. *Plant, Cell and Environment*.

Tyree, M.T. & Sperry, J.S. (1989) Cavitation and Embolism. *Water*, 19–38.

Walker, B.H., Ludwig, D., Holling, C.S. & Peterman, R.M. (1981) Stability of semi-arid savanna grazing systems. *The Journal of Ecology*, 69, 473.

Walter, H. (1971). Ecology of Tropical and Subtropical Vegetation.

Ward, D., Wiegand, K. & Getzin, S. (2012). Walter's two-layer hypothesis revisited: back to the roots! *Oecologia*, 172(3), 617–630.

Weiher, E. & Keddy, P. (2001). *Ecological assembly rules: perspectives, advances, retreats*. Cambridge: Cambridge University Press.

Wolf, A., Anderegg, W.R.L. & Pacala, S.W. (2016) Optimal stomatal behavior with competition for water and risk of hydraulic impairment. *Proceedings of the National Academy of Sciences of the United States of America*, 113, E7222–E7230.

Wolkovich, E.M. & Cleland, E.E. (2011) The phenology of plant invasions: a community ecology perspective. *Frontiers in Ecology and the Environment*, 9, 287–294.

Wright, S.J. & van Schaik, C.P. (1994) Light and the phenology of tropical trees. *American Naturalist*, 143, 192–199.

Yu, K. & D'Odorico, P. (2015) Hydraulic lift as a determinant of tree-grass coexistence on savannas. *New Phytologist*, 207, 1038–1051.

SUPPORTING INFORMATION

Additional supporting information may be found in the online version of the article at the publisher's website.

How to cite this article: Levine, J.I., Levine, J.M., Gibbs, T. & Pacala, S.W. (2022) Competition for water and species coexistence in phenologically structured annual plant communities. *Ecology Letters*, 25, 1110–1125. Available from: <https://doi.org/10.1111/ele.13990>

